

## Accepted Manuscript

### International Journal of Structural Stability and Dynamics

Article Title: Computation-effective structural performance assessment using Gaussian Process-based finite element model updating and reliability analysis

Author(s): Hans Moravej, Tommy H. T. Chan, Andre Jesus, Khac-Duy Nguyen

DOI: 10.1142/S0219455420420031

Received: 30 September 2019

Accepted: 03 June 2020

To be cited as: Hans Moravej *et al.*, Computation-effective structural performance assessment using Gaussian Process-based finite element model updating and reliability analysis, *International Journal of Structural Stability and Dynamics*, doi: 10.1142/S0219455420420031

Link to final version: <https://doi.org/10.1142/S0219455420420031>

This is an unedited version of the accepted manuscript scheduled for publication. It has been uploaded in advance for the benefit of our customers. The manuscript will be copyedited, typeset and proofread before it is released in the final form. As a result, the published copy may differ from the unedited version. Readers should obtain the final version from the above link when it is published. The authors are responsible for the content of this Accepted Article.

# Computation-effective structural performance assessment using Gaussian Process-based finite element model updating and reliability analysis

Hans Moravej<sup>1,\*</sup>, Tommy H. T. Chan<sup>1</sup>, Andre Jesus<sup>2</sup>, Khac-Duy Nguyen<sup>1</sup>

<sup>1</sup> School of Civil Engineering and Built Environment, Faculty of Science and Engineering, Queensland University of Technology (QUT), Brisbane, QLD, Australia

<sup>2</sup> Faculty of Environment and Technology, University of the West of England, Bristol, United Kingdom

\* h.moravej@qut.edu.au

## Abstract

Structural health monitoring data has been widely acknowledged as a significant source for evaluating the performance and health conditions of structures. However, a holistic framework that efficiently incorporates monitored data into structural identification and, in turn, provides a realistic life-cycle performance assessment of structures is yet to be established. There are different sources of uncertainty, such as structural parameters, computer model bias and measurement errors. Neglecting to account for these factors result in unreliable structural identifications, consequent financial losses, and a threat to the safety of structures and human lives. This paper proposes a new framework for structural performance assessment that integrates a comprehensive probabilistic finite element model updating approach, which deals with various structural identification uncertainties and structural reliability analysis. In this framework, Gaussian process surrogate models are replaced with a finite element model and its associate discrepancy function to provide a computationally efficient and all-round uncertainty quantification. Herein, the structural parameters that are most sensitive to measured structural dynamic characteristics are investigated and used to update the numerical model. Sequentially, the updated model is applied to compute the structural capacity with respect to loading demand to evaluate its as-is performance. The proposed framework's feasibility is investigated and validated on a large lab-scale box girder bridge in two different health states, undamaged and damaged, with the latter state representing changes in structural parameters resulted from overloading actions. The results from the box girder bridge indicate a reduced structural performance evidenced by a significant drop in the structural reliability index and increased probability of failure in the damaged state. The results also demonstrate that the proposed methodology contributes to more reliable judgement about structural safety, which in turn enables more informed maintenance decisions to be made.

## 1. Introduction

Civil infrastructure is a keystone in the evolution of a nation's safety and welfare. Currently, many structures and infrastructure do not meet the necessary levels of productivity and require maintenance and retrofitting. Decision-makers who are responsible for maintaining and upgrading the condition of civil engineering infrastructure must develop the most accurate and optimal maintenance strategies to efficiently use their available budget and resources. A significant tool for monitoring the safety of a structure over its

functional life is structural performance assessment. This plays an essential role in decision-making in terms of investigating infrastructure safety and selecting the most efficient long-term maintenance techniques.

In some cases, major maintenance may be expensive to perform and, depending on the extent of the maintenance (i.e., the level of required restoration), it may be cheaper to replace the entire structure. In addition, when a decision is made to perform repair and retrofit tasks, the structure will be non-operational and need to be evacuated for a period, causing inconvenience for residents—this is what happened in Sydney's Opal Tower in 2019, causing significant problems for the building's residents and the city council (Bolton, 2019).

Among the several indices used for structural performance assessment, such as risk, hazard and redundancy, the reliability index is the most commonly deployed for civil engineering structures. Structural reliability analysis plays an essential role in decision-making for investigating infrastructure safety and choosing the most efficient long-term maintenance techniques for a structure. In general, a lifetime structural reliability analysis is conducted to investigate the performance of a structure over time, and integrates the probability of failure with the total cost expected to be accrued over the structure's entire life cycle. The reliability analysis can be applied to either individual structural components or the entire structure as a system. While component reliability methods, such as the member replacement method (Hendawi & Frangopol 1994) and the unzipped method (Thoft-Christensen & Murotsu 1986), may be applicable to mechanical structures, they have not been proven practical for implementation in complex and large-size civil structures. Further, system reliability methods provide greater insight into possible scenarios for the failure of structures (Moses, 1982; Moses & Rashedi 1983; Tang & Melchers 1988; Okasha & Frangopol 2010).

Most previous studies on the performance assessment of civil structures have been based on the structural condition in the design stage (Akgül & Frangopol 2005; Moravej et al. 2016; Moravej & Vafaei 2019). To compute system reliability, Estes and Frangopol (1999) and Akgül and Frangopol (2004a, 2004b & 2005) have used the American Association of State Highway and Transportation Officials guidelines to formulate limit-state functions for the components of various bridge systems in different failure modes. The incremental finite element (FE) analysis approach to computing the system reliability of structures has demonstrated better outputs among other current methods and shows the appropriate functionality of civil structures. This approach allows the resistance of the entire system to be predicted since all the components act together under given loading cases (Okasha & Frangopol 2010). The reliability analysis of structures during their service lives has been mostly directed by predicting conditions from the design stage to different structural ages by applying empirical models, such as Nowak's (1999) section-loss-due-to-corrosion model. As with any empirical model, such models have degrees of inaccuracy that must be validated by inspecting real structural conditions for optimal decision-making regarding maintaining and retrofitting structures—otherwise, a significant budgetary loss arising from faulty state prediction is highly probable. According to estimations by the American Society of Civil Engineering (ASCE), in the United States alone, the appointed fund for upgrading the nation's infrastructure rose from \$1.6 trillion in 2005 to \$2.2 trillion in 2009 (ASCE, 2010). Therefore, any decision about infrastructure maintenance must be based on realistic structural identification.

This hurdle can be addressed through non-destructive testing (NDT) to enable more trustworthy predictions to be made about a structure's condition over a specific interval during its lifespan. However, NDT's functionality is not particularly broad; it is limited to assessing small structures or components. Further, NDT is ineffective in cases where components are inaccessible. An entire structure's true performance can be evaluated by accurately assessing its structural system reliability (Estes & Frangopol 1999).

In the last two decades, structural health monitoring (SHM) has provided widespread identification of the current state of structures (as-is) as entire systems. However, a gap exists between information obtained

from SHM and structural performance assessment. While SHM mostly concentrates on damage evaluation, structural performance assessment is focused on addressing the serviceability and safety of structures. In addition, methods are lacking for processing raw data obtained from SHM and making that data functional for validating and updating structural reliability.

For the first time, Hosser et al. (2008) have proposed a basis for integrating SHM into a reliability-based system assessment of structures. Recently, with the emergence of finite element model updating (FEMU) as one application of SHM, it has been possible to calibrate the numerical models of structures during their lifespans and match these to real structures in their current states as it has been presented in the research by Kodikara et al. (2016), Nguyen et al. (2018) and Nguyen et al. (2019). Accordingly, the updated numerical models can be subsequently applied to update lifetime structural reliability. FEMU is a process in which the input parameters of the finite element (FE) models of structures are tuned so that the responses obtained from the finite element analysis agree with those measured from the test (Moravej et al. 2017; Moravej et al. 2019a). Hence, applying FEMU means that the current condition of structures can be realised and, consequently, that structural performance can be predicted more confidently, since FEMU's judgement is tuned to structures' actual behavior based on their as-is conditions. Further, when applying FEMU, structural performance can be obtained for the entire system, where all components are acting together under a given loading case, and not merely for a single component. Assessing the life-cycle performance of structures can be carried out in two categories: point-in-time (instantaneous) and cumulative-time-dependent. Analysis in the first category at each time depends only on the existing states of the physical parameters without taking into account the previous conditions, and time is considered a fixed variable. Conversely, time-dependent reliability of structures not only considers both the randomness of resistance and the stochastic nature of the load, but also regard time as a random variable, and is performed to predict the remaining service life of structures (Enright & Frangopol 1998; Mori & Ellingwood 2006).

Recently, researchers have attempted to link FEMU with structural life-cycle performance monitoring. However, most have employed deterministic approaches, such as particle swarm optimisation (Okasha et al. 2012). Nevertheless, FEMU is susceptible to several sources of uncertainty, such as structural parameters, computer model bias and measurement errors, that could affect the results of its calibration, and consequently affect the accuracy of the sources used for structural performance assessment. Therefore, more accurate FEMU leads to more reliable performance assessments of structures and, as a result, more confident decision-making concerning maintenance and structural safety. While deterministic FEMU techniques are generally computationally efficient, they are susceptible to an ill-conditioning problem and rarely consider uncertainty in their identifications (Friswell & Mottershead 2013). Among deterministic methods, fuzzy approach considers uncertainties in input parameters; however, this approach applies the Min-Max composition between the fuzzy modeling and the input, and just yields a worst-case scenario as dependencies between model parameters and experimental data cannot be clearly identified (Simoen et al. 2015; Pan & McMichael 1998). Also, the fuzzy-based methods' outputs are in the form of a fuzzy sets, which is less intuitive to be interpreted and complicated to use in a reliability analysis (Baraldi et al. 2015). Further, while a fuzzy approach considers the uncertainty in input parameters, it is unable to account for uncertainty from model bias.

Against with deterministic techniques, probabilistic approaches, such as the Bayesian approach account for uncertainties in the updating process comprehensively. However, this also increases computational costs, and rendering such techniques would be impractical for complex structures. Recently, surrogate models (metamodels) such as Kriging or Gaussian Process (GP) models have been proposed to reduce the computational cost of analysis. Nannapaneni and Mahadevan (2016) proposed a probabilistic framework to include model uncertainty with application of first-order reliability method (FORM) and GP. Other studies of GP-based methods comprise the efficient global reliability analysis method developed by Bichon et al. (2008), the Adaptive Kriging Monte Carlo simulation method proposed by Echard et al. (2011), joined adaptive Kriging and importance sampling (Dubourg et al. 2013; Echard et al. 2013). Jiang et al. (2013)

applied a GP modeling to correct a bias function and quantify model uncertainty based on one accurate model of a vehicle. In another attempt, uncertainty from an inadequate model of a real physical system has been addressed through integrating the model bias into reliability-based design optimization and the results were verified by two vehicle models (Pan et al. 2016).

Accordingly, this paper proposes a structural performance assessment approach, integrating a modular Bayesian approach (MBA) into structural reliability analysis. For the first time, this research develops a framework for evaluating structural performance based on a reliable FE model updating that considers various sources of uncertainties and is computationally efficient. Unlike the fully Bayesian approaches, which try to solve a problem in one attempt, MBA splits the problem into four modules, making the process more efficient. In addition, this method considers uncertainty more comprehensively than previous probabilistic techniques. MBA uses a GP to substitute the simulated model and discrepancy function by estimated metamodels.

Regarding reliability analysis, the FORM, which is known as the most common technique in civil structural engineering, is used in this research. The calibrated numerical model obtained from MBA, which is well-matched to the reality, is deployed to realize structural performance. Accordingly, the loading demand and capacity of structures can be obtained from the updated numerical models and the performance function can be generated between them. Then, reliability analysis is performed to calculate the performance function and find the reliability index and probability of failure. Against with previous research, which has mostly used reliability analysis in the ultimate limit state (ULS), this study targets the serviceability limit state (SLS), since preventive maintenance is effective when it is applied in SLS before a significant damage occurs.

Another contribution of this study is that the applicability of the proposed framework is investigated on a large lab-scale box girder bridge (BGB) in two states: undamaged and damaged. The damaged state is applied in a controlled laboratory environment in a way that corresponds with typical effects of impact or ageing in structures. This study seeks to understand the extent to which structural performance is degraded at various levels of structural condition, and the findings will play a significant role in planning maintenance schedules and ensuring structural safety.

## 2. Finite element Model Updating

This section refers to the model updating technique applied in this work. An approach to incorporate uncertainty in different stages of a FEMU process will be briefly described. For more details of the approach, refer to Moravej et al. (2019a & 2019b). The comprehensive relation between observations (i.e., measured structural response) and a numerical model can be stated in Eq. 1

$$y^e(\mathbf{x}) = y^m(\mathbf{x}, \boldsymbol{\theta}) + \delta(\mathbf{x}) + \varepsilon \quad (1)$$

where  $\boldsymbol{\theta}$  is a vector of structural parameters needed to be calibrated, and  $\mathbf{x}$  are the design variables such as temperature, wind speed, and applied force;  $y^e(\mathbf{x})$  represents the experimental response such as natural frequency and mode shape;  $y^m(\mathbf{x}, \boldsymbol{\theta})$  denotes the corresponding computer model response;  $\delta(\mathbf{x})$  is the discrepancy function, which stands for misfit between measured response and simulated counterpart due to assumptions and simplifications made during developing the computer model, such as the assumption of linearity and homogeneity of material behavior; and it varies with experimental design variables since these variables may affect the measured and simulated responses differently. Also,  $\varepsilon$  accounts for the

experimental uncertainty, and denotes variations that may occur in the experimental measurement even when the test is repeated with the same settings. Because this equation accounts for different sources of uncertainty, it is considered as a comprehensive formulation for structural design under uncertainty. In fact, there is additional uncertainty associated with missing data (observed or simulated) as only a limited set of simulation and experimental data at discrete locations can be obtained, in which an analyst needs to interpolate or extrapolate to estimate the response at other regions. Hence, this source of uncertainty is denoted as interpolation/extrapolation uncertainty. It is worth noting that this kind of uncertainty would vanish by applying a FE model since it is able to simulate the physical model entirely over a spaced grid covering the input domain. However, in cases of complex structures, computer models are cumbersome to run and interpolation uncertainty becomes relevant during model updating. The model updating approach by Kennedy and O'Hagan (2001) is one such approach, against many others, which integrates both a discrepancy function and calibration parameters. However, it was not effective in targeting identifiability, which refers to the ability to predict the true values of the model parameters and actual modeling error based on the available data (Arendt et al. 2012a). Arendt et al. (2012b) improved Kennedy and O'Hagan's original method by applying an MBA to rectify the identifiability concern using a more informative model, based on regression of multiple responses. This method substitutes a Gaussian process (GP) model with FE model, which is a surrogate model. It has been observed that the method considerably decreases computational effort, and it is believed to be the most appropriate approach to update a FE model under uncertainty (Conde et al. 2018; Jesus et al. 2014; Jesus et al. 2017; Jesus et al. 2019a; Jesus et al. 2019b; Lophaven et al. 2002). The GP model for interpolation/extrapolation with the capability for addressing uncertainties is found to be effective, even with limited data. This formulation is more advantageous than the other related studies in model updating as it involves the main sources of uncertainties, which eventually provides more realistic outcomes.

## 2.1 Gaussian Process metamodel

For a GP approach, it is assumed the response surface  $y^m(\mathbf{x}, \boldsymbol{\theta})$  in Eq. 1 is a single point of a spatial random process (e.g. Gaussian) with a prior mean function and a covariance function. By means of interpolations and extrapolations, this approach provides a predicted GP fitted on entire observation points by assuming that the metamodel of model  $y^m$  is a single point of a spatial random process (O'Hagan, 2006). To characterize a GP, its prior mean function and prior covariance function should be identified. It should be noted that such mean function and covariance function comprise hyperparameters such as vector of regression functions and vector of coefficients, which should be identified. In other words, one GP can be identified by finding its mean function and covariance functions' hyperparameters (Arendt et al. 2012a). After obtaining the hyperparameters of the prior functions, two methods are widely used to estimate the GP. In practice, for computational reasons, it is recommended to calculate the maximum likelihood estimates (MLEs). In contrast, a Bayesian approach, as the other method, calculates an entire posterior distribution for the hyperparameters which is computationally expensive.

## 2.2 Modular Bayesian Approach (MBA)

MBA, against with fully Bayesian approach, separates the updating process into four steps (modules) to reduce the computational cost. Herein, the hyperparameters of the GP are estimated separately and sequentially (Arendt et al. 2012a). In this approach, at first, several data set from a computer model is prepared. The number of data set depends on the size of the structure, the number of calibration parameters and structural responses.

In application of MBA, GP models are replaced with the numerical model, experimental response and discrepancy function. Following the relation between the observations and the numerical model shown in Eq.1, the GP model for an experimental response  $y^e(\mathbf{x})$  is the summation of the GP models for a discrepancy function  $\delta(x)$  and a computer model  $y^m(\mathbf{x},\boldsymbol{\theta})$ . Subsequently, this GP model will be applied to find the experimental response at any  $x$ . Therefore, in the first module, a GP is replaced with the simulated model; and to estimate its hyperparameters, the GP model will be fitted to pass through all simulation data point.

In the second module, by using the simulation data, the measured experimental data and the estimates of the hyperparameters from module 1 and the prior for the calibration parameters, hyperparameters of the GP model for discrepancy function are obtained.

In the third module, the posterior distribution of the calibration parameters is calculated based on the experimental data, the simulations data, and the estimated hyperparameters from modules 1 and 2. The posterior distribution is obtained by using Bayes theorem as expressed as follows:

$$p(\boldsymbol{\theta}|\mathbf{d},\boldsymbol{\Phi}) \propto p(\mathbf{d}|\boldsymbol{\theta},\boldsymbol{\Phi})p(\boldsymbol{\theta})(2)$$

Where  $\boldsymbol{\Phi}$  is denoted as the estimates of hyperparameters of model and discrepancy;  $\mathbf{d}$  stands for all experimental and numerical responses;  $p(\boldsymbol{\theta})$  is the prior distribution of the calibration parameter vector  $\boldsymbol{\theta}$ . It is worth noting that the posterior distribution of  $\boldsymbol{\theta}$  and the hyperparameter estimates from modules 1 and 2 influence the prediction of the experimental response. After gathering the experimental and simulation data and obtaining the hyperparameters in the first and the second module, and by applying a specific value of  $\boldsymbol{\theta}$ , the conditional posterior distribution of the experimental response can be obtained at any point  $\mathbf{x}$ , with mean and covariance functions. Consequently, the posterior distribution of the experimental response involves all sources of uncertainty, including parameter uncertainty, model discrepancy, interpolation uncertainty and experimental uncertainty.

In the fourth module, the measured responses are using the test data, estimated hyperparameters and updated parameters obtained from modules 1, 2 and 3, respectively. In this module, the posterior response from updated model as well as the updated discrepancy function can be resulted (Arendt et al. 2012a). For the estimation of the responses, 40 test data points for the undamaged state and 60 test data points for the damaged state are randomly distributed among the simulated data points. It is worth noting that simulated data points have been collected using Latin Hypercube Sampling (LHS) approach. In addition, it is assumed that the measured responses are independent of time, temperature variation, and other operational effects.

### 3. Structural Reliability Analysis

The calibrated numerical model in the previous stage of this framework is applied to investigate the performance of structure in its current condition by using reliability analysis. In general terms, structural reliability theory regards all basic variables, such as loading conditions, material and geometrical properties, as random with specifying their probability distributions obtained from the research background or by applying tests. In regard to computing structural reliability, performance function  $Z$  for each limit state can be generated as follows:

$$Z = R - E(3)$$

The above expression illustrates the relation between the resistance of structure,  $R$ , and the action effect that applies to the structure,  $E$ . The fundamental task of structural reliability is to provide the conditions for the following requirement:

$$E < R \quad (4)$$

This requirement defines an acceptably safe state for a structural system. It is supposed that structural failure happens when the requirement is not fulfilled. Accordingly, an expected threshold between the circumstances for the safety and failure of a structure is specified as:

$$Z = R - E = 0 \quad (5)$$

This equation denotes a fundamental formula for the margin of failure in performance, which can be constructed for both ultimate and serviceability limit states. In reliability analysis, the variables  $E$  and  $R$  are random variables, so the validity of inequality in Eq. 4 cannot be confirmed with 100% confidence. Thus, it is necessary to consider the circumstances in which the limit state designated by Eq. 4 may be exceeded and the failure occurs with a certain probability. The principal target of the theory of reliability is the evaluation of the probability of failure  $P_f$ . For the state of inequality in Eq. 4, the probability of failure will be accordingly written as Eq. 6.

$$P_f = P(E > R) \quad (6)$$

The random nature of the load action effect and the resistance is denoted in terms of suitable parameters such as force, strain and deflection, which are generally defined by the applicable distribution functions  $\phi E(X)$  and  $\phi R(X)$ , respectively, where  $\mathbf{X} = (X_1, X_2, \dots, X_n)$  represents the random variables such as deflection or normal stress. The distribution  $\phi E(X)$  and  $\phi R(X)$  are presented in Fig. 1.

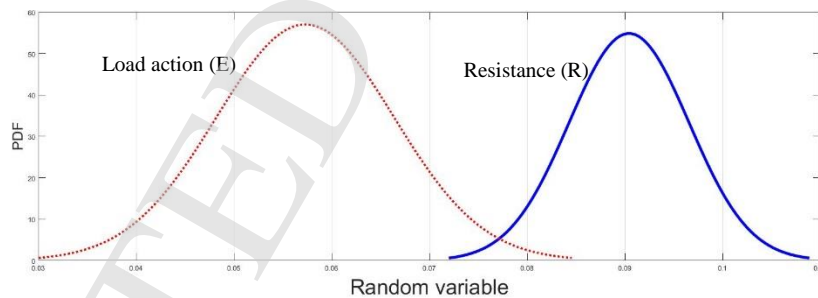


Figure 1. Distribution of Load action and Structural resistance

As illustrated in the figure, two distribution functions overlap each other in one region; hence, unsatisfactory recognition of  $E-R$  relation can occur if the load action is larger than the resistance, and the failure is expected.

Apparently, to preserve the probability of failure  $P_f$  within adequate limits, the distributions of  $E$  and  $R$  need to fulfil certain conditions. Therefore, Eq. 6 for the probability of failure is reformed as Eq. 7, as follows:



$$P_f = P(E > R) = P(Z < 0) = \int_{Z(X) < 0} K(X) dx \quad (7)$$

Here,  $K(X)$  is the joint PDF of  $X$ . Since the direct calculation of the integration is computationally expensive and beyond engineering applicability, analytical techniques to solve the problem are not effective. It is also unfeasible to perform numerical techniques to find an answer as a result of high levels of dimensionality in engineering practice. So the application of approximation techniques is required.

### 3.1 First-Order Reliability Method (FORM)

FORM is the most applicable approximation technique in structural reliability, which makes the probability integration to be solved by simplifying the integrand  $K(X)$  and approximating the integration boundary  $Z(X) = 0$  by using the first-order Taylor series expansion (Hasofer and Lind 1974). This simplification is applied through the conversion of an original, random space into a standard normal distribution space from  $X$  to  $U$ . This type of conversion is carried out by using Rosenblatt's transformation, which requires the cumulative distribution function (CDF) of a random variable is remained unchanged after the transformation. The transformation is expressed as follows:

$$K(X_i) = \phi(u_i) \quad (8)$$

Here,  $\phi(u_i)$  is the CDF of standard normal distribution. Then, the transformed standard normal variable is shown by Eq. 9.

$$u_i = \Phi^{-1}[K(X_i)] \quad (9)$$

It should be mentioned that after the transformation, the formulation of the performance function  $Z(X)$  will transform into  $Z(U)$ , and in turn, the probability of failure is calculated by the following equation:

$$P_f = P\{Z(U) < 0\} = \int_{Z(U) < 0} \phi_u(u) du \quad (10)$$

Here,  $\phi_u(u)$  is the joint PDF of  $U$ , which is the product of the individual PDFs of standard normal distribution.

It is worth noting that this transformation does not affect the accuracy since the integration in  $U$ -space shown in Eq. 10 is the same as that in  $X$ -space of Eq. 7. This transformation makes the contours of the integrand in standard normal distribution a concentric circle, which is easier to be integrated. FORM also approximates the integration boundary  $Z(U) = 0$  by applying the first-order Taylor series expansion as illustrated in the following expression:

$$Z(\mathbf{U}) \approx Z(\mathbf{u}^*) + \nabla Z(\mathbf{u}^*) (\mathbf{U} - \mathbf{u}^*)^T \quad (11)$$

while  $\mathbf{u}^* = (u_1^*, u_2^*, \dots, u_n^*)$  is the expansion point of  $\mathbf{U}$  on the boundary  $Z(\mathbf{U}) = 0$ ,  $\nabla Z(\mathbf{u}^*)$  stands for the gradient of  $Z(\mathbf{U})$  at  $\mathbf{u}^*$ . To achieve the highest accuracy in the approximation, the performance function  $Z(\mathbf{U})$  is extended to reach the point that has the highest probability density (HPD), which has the maximum value of the integrand. Thus, the performance function will be approximated at HPD. The position of HPD is obtained by maximizing the joint PDF  $\phi_u(\mathbf{u})$  at the boundary of the performance function (i.e.,  $Z(\mathbf{U}) = 0$ ).

In other words, the HPD is the shortest distance from the limit state  $Z(\mathbf{U})=0$  to the origin in  $\mathbf{U}$ -space, and this is called reliability index  $\beta$ .

Accordingly, the probability of failure can be calculated by the following equation (Du, 2005):

$$P_f = \Phi(-\beta) \quad (12)$$

If the parameters representing the action effect  $E$  and the resistance  $R$ , respectively, have normal distributions,  $\beta$  can be obtained as:

$$\beta = \frac{\mu_Z}{\sigma_Z} \quad (13)$$

where  $\mu_Z = \mu_R - \mu_E$ , and  $\sigma_Z = \sqrt{\sigma_R^2 + \sigma_E^2 + 2\rho_{RE}\sigma_R\sigma_E}$

$\mu_R$  and  $\mu_E$  are mean values of  $R$  and  $E$  and  $\sigma_R$  and  $\sigma_E$  are standard deviations of  $R$  and  $E$  respectively.  $\rho_{RE}$  is the correlation coefficient between  $R$  and  $E$ . If the parameters representing the action effect and the resistance are not normal distributions, the distribution of the safety margin  $Z(\mathbf{U})$  is not a normal distribution as well. In this case, numerical integration or transformation from different distributions into normal distribution can be applied for these parameters.

Accordingly, in this research, the updated FE model of structure is employed for updating the structural capacity in its current state. FORM is applied to calculate the performance function in any limit state, and provides structural reliability index and probability of failure.

The research framework in this study is illustrated in Fig. 2. As shown in the flowchart, the methodology comprises three main steps.

The first step, pre-updating, provides the data sets from both counterparts, the experimental test and numerical model of structures, and confirms if launching the FEMU process is acceptable or not from assessing the provided data sets. The correlation analysis in the first step is used to ensure that the initial FE model represents the main characteristics of the experimental one, and that the difference between them is within a reasonable range, for which the FE model is updateable. For example, if the initial correlation analysis results in a big discrepancy between the two counterparts, the FE model should be improved before carrying out model updating process in the later stage.

In this study, error in natural frequency is used to analyze the correlation level between the FE model and experimental one as this is a global parameter and represents central effect of all structural parameters. Apart from this index, one can use the errors in other vibration measures such as Frequency Response Functions (FRFs) and mode shape (Moravej et al. 2017).

The second step engages with the comprehensive FEMU approach to calibrate the numerical models of structures with respect to their current conditions and available uncertainties.

In the third step, the updated structural numerical model obtained in the second step is applied to obtain the current structural capacity (as-is) and loading demand to evaluate structural performance using structural reliability analysis.

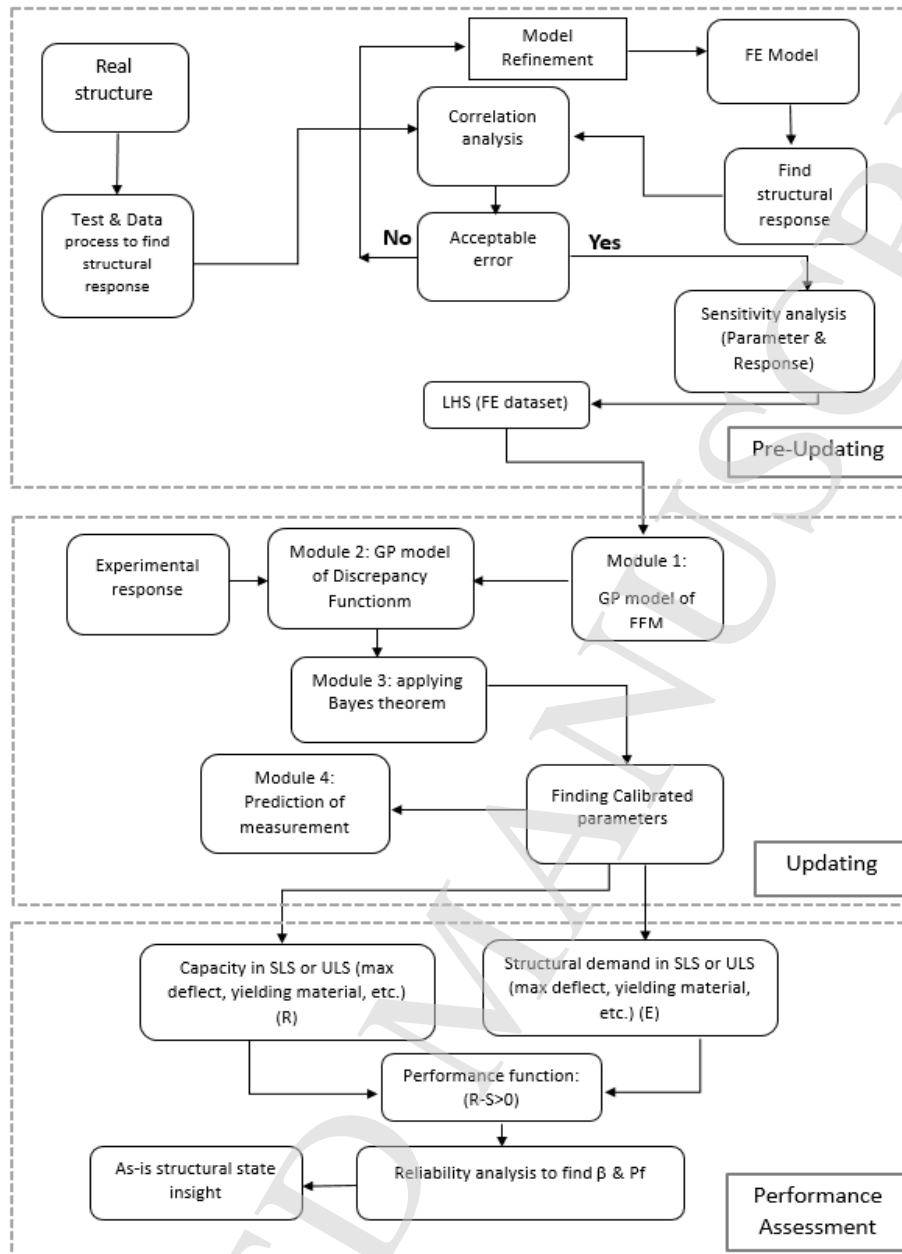


Figure 2. The flowchart of the research framework

#### 4. Step-by-step Application of the Methodology to a large lab-scale concrete structure

In this study, the performance of a box girder bridge (BGB) has been inspected in two states: undamaged and damaged phases. The BGB represents a typical in-service hollow-core bridge deck in Australia. It is 6 m long, and its cross section consists of three parts that were cast separately as the top slab, the bottom slab, and the two parallel webs. The geometry of the BGB and properties of the materials used in construction of the structure are presented in Fig. 3 and Table 1, respectively.

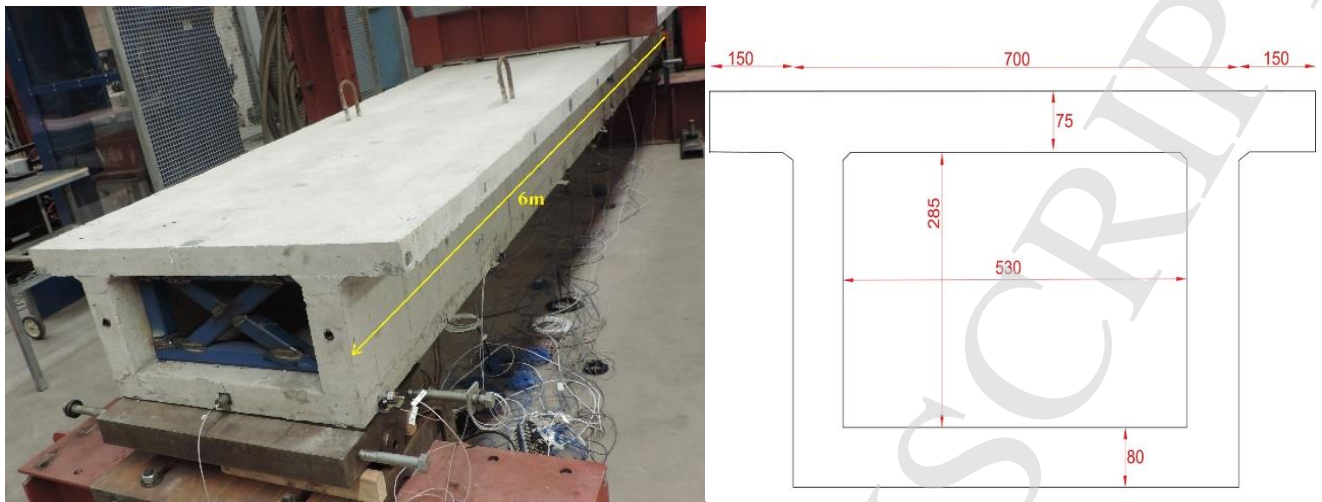


Figure 2. The dimensions of Box Girder Bridge

Table 1 Material properties used in FE model of the BGB

Parameter	Material	Nominal value
Young Modulus E (GPa)	Concrete	32
	Reinforcement	200
Mass Density $\rho$ (Kg/m <sup>3</sup> )	Concrete	2400
	Reinforcement	7850

More information about the fabrication process can be found in Pathirage (2017). The bridge model is simply supported at its two ends using roller and pin supports, as illustrated in Fig. 4.

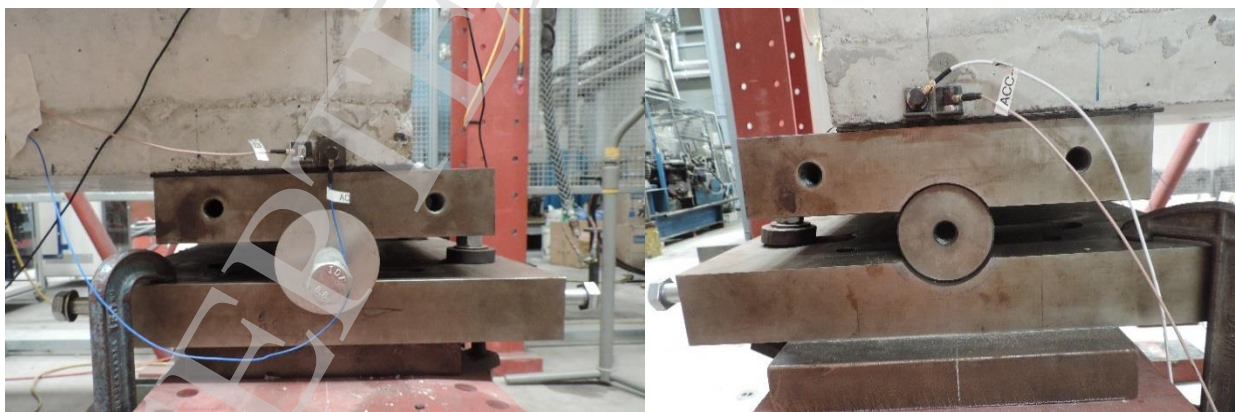


Figure 3. Simple supports of Box Girder Bridge as Roller (left) and Pin (right)

The initial condition of the structure is considered as the undamaged state, in spite of some minor cracks observed on the bottom slab. The damaged state represents the condition after a point load together with a cyclic load were applied at the mid-span and generated some cracks as shown in Fig. 5. It is worth noting that each crack runs almost across the whole cross section, throughout the whole bottom flange and most of the webs. The region of cracks covers half of the beam span, from  $\frac{1}{4}$  from the left support to  $\frac{1}{4}$  from the right support.

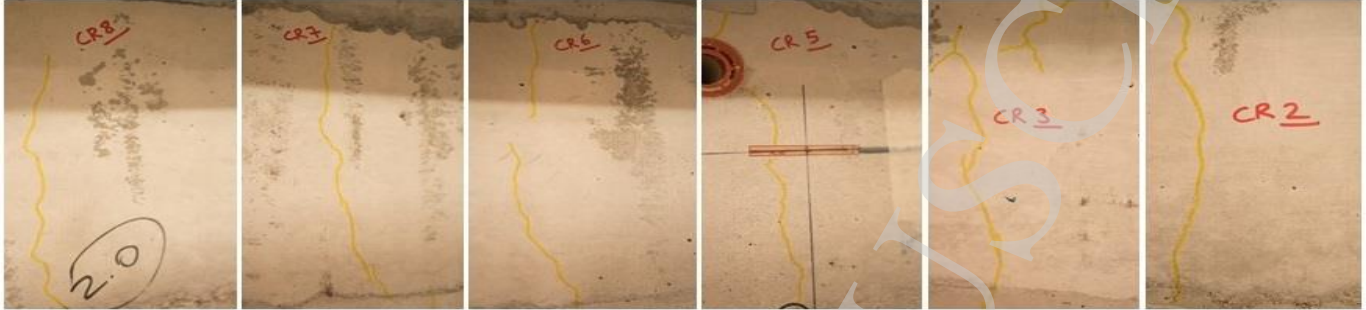


Figure 4. Generated cracks on the body of BGB in damaged state

In the forthcoming subsections, a FE model of the BGB and the applied modal analysis are described. Then, the application of the FEMU in both states is highlighted. Finally, a reliability analysis of the BGB is performed.

#### 4.1 Construction of FE model of Box Girder Bridge

The structural details of the BGB, such as material and geometrical properties and support conditions were chosen according to the design details and applied to build an initial FE model using ABAQUS software package (ABAQUS, 2017). The T3D2 truss and C3D8R solid elements from the ABAQUS library were selected for the reinforcement and concrete elements, respectively. The modulus of elasticity ( $E$ ) was selected as 32 GPa for concrete and 200 GPa for reinforcement. The mass density ( $\rho$ ) was considered as 2,400 kg/m<sup>3</sup> for concrete, and 7,850 kg/m<sup>3</sup> for reinforcement. Moreover, the boundary conditions were simulated as simple supports with full fixity in vertical displacement at both ends and horizontal displacement at the pin support. Regarding mesh size selection, a convergence assessment of displacement for different mesh sizes was implemented through the application of a load at the mid-span. As a result, 50mm mesh grids were found to be sufficient for this model. In this study, four natural frequencies shown in Fig. 6, including the first and the second vertical bending, the first lateral bending, and the third vertical bending modes, were chosen as the structural responses to be applied to the model updating process since these vibration modes matched well with the modes obtained from the measured data described in the following section. More details of the analysis can be found in Jamali et al. (2018).

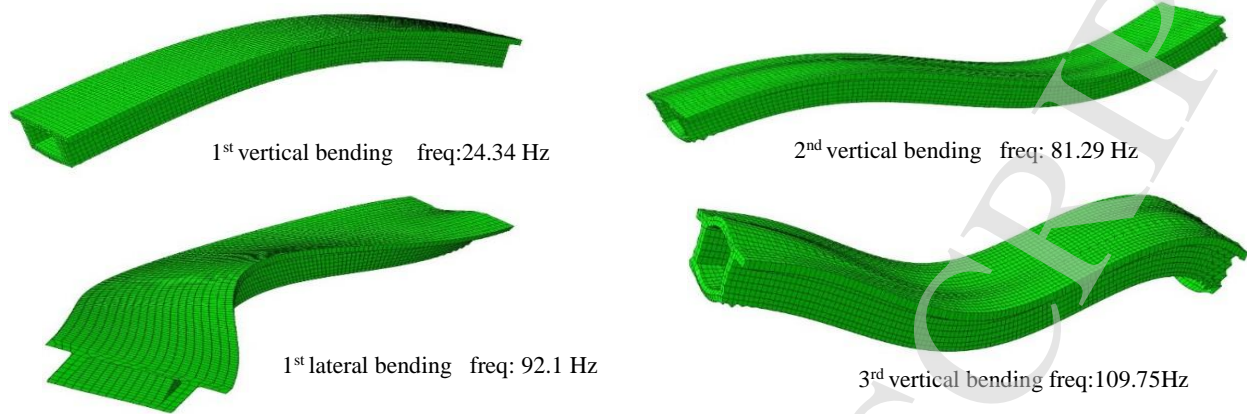


Figure 6. Numerical mode shapes used in FEMU

## 4.2 Modal Data Analysis

The primary measurements of responses used in the previous studies on finite element updating are mostly vibration data (Okasha & Frangopol, 2012). It is reasonable to select global responses for applying in FEMU which are affected by the overall resistance of the structure. In this study, the BGB was subjected to a random excitation by applying an impact hammer at multiple locations. Vibration data points have been collected using a data acquisition setup. The acceleration responses of the structure in the two states were recorded and applied in the FEMU process. The applied sensory system for this work can be found in Moravej et al. (2019a) and Nguyen et al. (2017). Prior to select an accurate sensor arrangement, different features have been noted, such as the type and number of existing sensors, the required quantity of channels in the data acquisition set, and the excitation resource. A stochastic subspace identification method has been used for post-processing of the measured accelerations in the modal analysis platform of the ARTEMIS software package (ARTEMIS, 2011). Fig. 7 presents an example of the modal analysis for a measured data set.

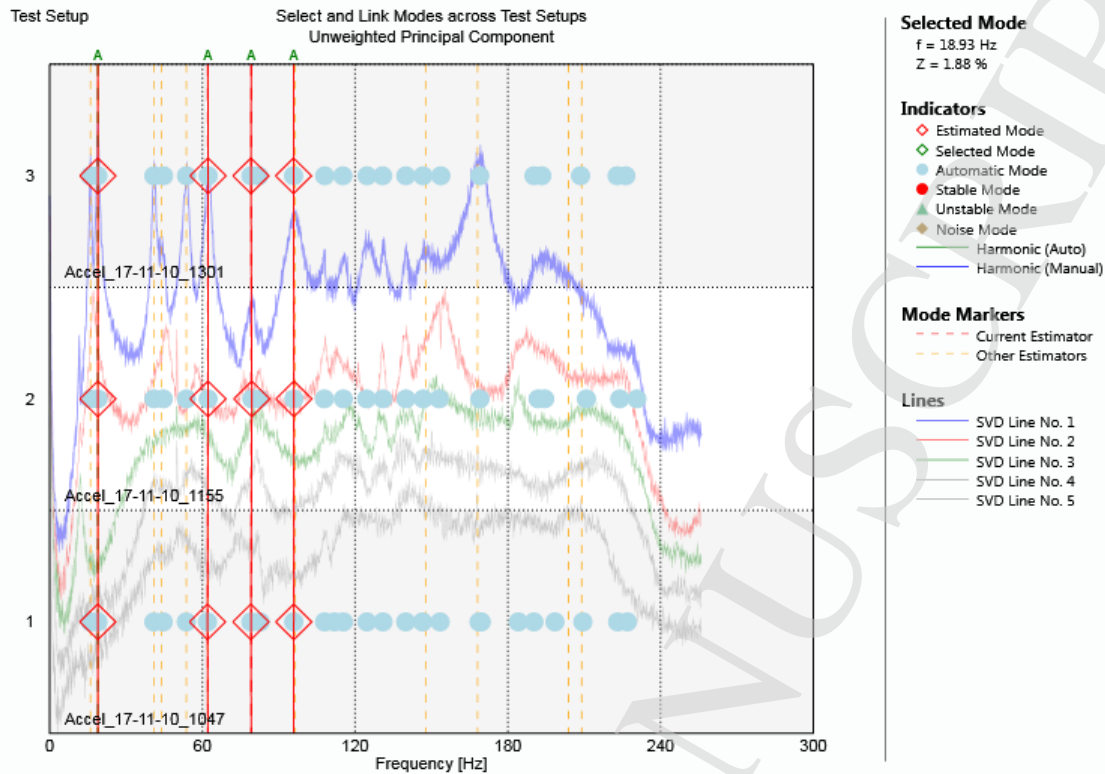


Figure 7. Capturing measured frequency through modal analysis in ARTeMIS

Since the test was performed in a controlled condition in the laboratory, the ambient properties could not significantly disturb the measured responses. Therefore, 40 datasets from the undamaged state and 60 datasets from the damaged state were found sufficient for the model updating process. From the measured natural frequencies, four modes similar to the simulated ones were picked for the FEMU practice. Naturally, the number of degree of freedoms (DOFs) in an experimental model differs from that of the FE model due to an inadequacy of existing sensors (Moravej et al., 2017). Addressing this mismatch, the method of coordinate expansion was performed to expand the DOFs of the experimental model to match those of the FE model (Moravej et al., 2017). Table 2 illustrates the natural frequencies of both states. The experimental mode shapes can be found in Moravej et al. (2019a).

Table 2. Experimental natural frequencies in two states

Mode order	Natural frequency (Hz) of undamaged state		Natural frequency (Hz) of damaged state	
	Mean	Standard Deviation	Mean (Hz)	Standard Deviation
1	21.65	0.106	18.78	0.082
2	67.06	0.21	63.06	0.174
3	84.32	0.124	80.73	0.14
4	98.21	0.18	95.74	1.023

### 4.3 Application of FEMU on the case study

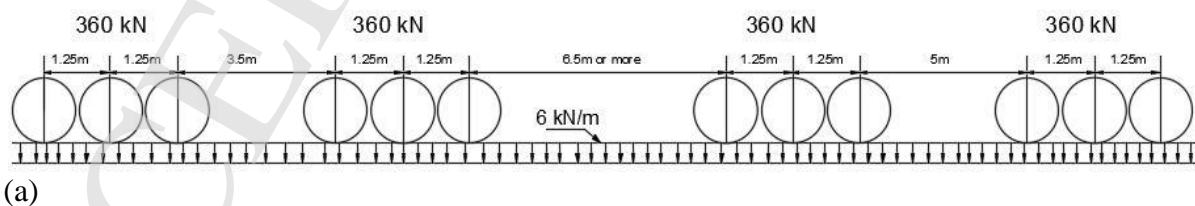
To commence the process of updating, sensitivity analysis has been applied to select the most sensitive parameters and responses. In relation to the experimental responses, the four modal frequencies were

nominated as sensitive responses. As mentioned before, in the initial FE model, both ends of the BGB were modeled as simple support with full fixity in vertical displacement. However, by correlating the modal shapes of the FE model and those of the experiment, it was observed that the roller in the experimental model exhibited a bouncing in the second and third vertical mode shapes, which dissatisfies the assumed fixity of the boundary conditions. Consequently, a more exact simulation of the boundary conditions is needed to accurately signify the behavior of the structure, so the vertical spring stiffnesses of the supports must be calibrated. For the process of updating, material properties were separated for three different parts, which are the bottom slab, the webs and the top slab. This is because the BGB was cast in the three corresponding stages. In addition, the health conditions visually observed for the three parts were different in the damaged state. Based on the sensitivity analysis, the five most sensitive parameters were selected as Young's moduli for the bottom slab, the webs, and the top slab ( $E_{cBot}$ ,  $E_{cWeb}$ , and  $E_{cTop}$ ), as well as the vertical spring stiffness coefficients of the two supports (Kroller & Kpin).

The drop in the number of parameters was sufficient to decrease the computational cost. It is worth noting that in the damaged state, the Young's moduli of the three parts would decrease and the boundary conditions of both supports would not be affected. At each state, an MBA is carried out to provide the calibrated parameters to be applied in the reliability analysis. Thus, in module 1 and 2, two GP metamodels are replaced with the FE model and the discrepancy function, respectively, and their hyperparameters are estimated accordingly. In module 3, given the GP models of FE model and discrepancy function from the previous modules, and by applying Bayesian approach and MCMC, the PDF of calibrated parameters are obtained.

#### 4.4 Reliability Analysis Application

In this study, to integrate the FE model into reliability analysis, the PDF of calibrated parameters was obtained at each state (undamaged and damaged) by applying an MBA, and used to quantify the probabilistic distribution of both structural resistance and load action effect arising from a moving load, which is a common demand applied to bridge structures. The moving load MS1600, as the most commonly used moving load specification in Australian bridge design code (AS5100.2, 2017), has been used in this study. This load specification comprises two different loading cases as M1600 and S1600, as shown in Fig. 8. The reliability analysis was conducted in an SLS, since, at both states, the structural materials were in the linear elastic region and had not yielded. Regarding the reliability analysis, two structural features, deflection and strain, were considered as the two separate variables in the performance function. The distribution types of applied loading cases were adopted from Nowak (1999). In this study, LHS was employed for the random sampling of the calibrated parameters and the loading case to obtain the distributions of the deflection and strain for each health state. LHS is an intelligent alternative to random sampling, a special kind of weighted random sampling which results in a better representative distribution of model outputs. Achieving the distribution of the variables in the performance function at each state, reliability analysis using FORM is then carried out to find the point-in-time structural performance. Accordingly, the reliability index and the probability of failure are provided at each state.





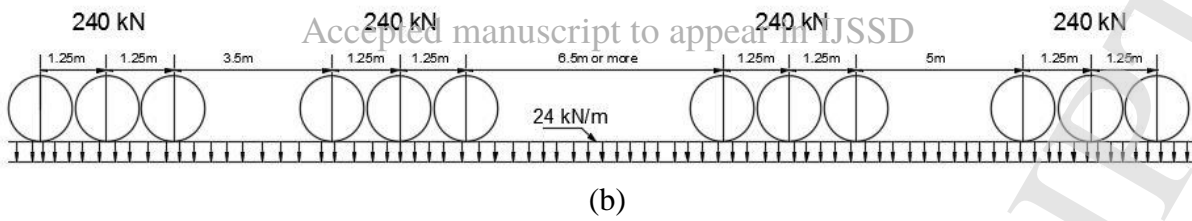


Figure 8. Applied moving load(MS1600) from Australian code (AS 5100): (a) M1600, (b) S1600

The loading cases to be applied to the BGB are downscaled by a factor of 0.04 according to Harris and Sabnis (1999). Maximum deflection and maximum normal strain have been selected in this study to address the effect of load action and structural resistance. Furthermore, incremental finite element analysis recommended by Okasha and Frangopol (2010), were applied in this study to obtain the resistant capacity. The analysis stops when a serviceability limit (i.e. the maximum deflection) is reached (AS 5100.2, 2017). The corresponding maximum normal strain at this increment is also recorded as the strain resistant of the structure. Consequently, the reliability analysis is conducted based on the changes in the two features. The analysis was repeated 200 times for each state with random sampling generated from the LHS. The number of iteration is concluded based on engineering judgment and according to the previous studies (Okasha & Frangopol 2012). Consequently, at each state, with obtaining the distribution of resistant capacity and the loading action, the performance equation is calculated using FORM to determine the reliability index, and in turn, the probability of failure.

## 5. Results and Discussion

The initial FE model of the structure has been calibrated for both states, undamaged and damaged, with the application of MBA and using the four natural frequencies as the responses. Bayesian approach, which its likelihood function contains the GP models of FE model and discrepancy function obtained in modules 1 and 2, is applied to estimate the posterior distribution of the updated parameters. Since multiple parameters are calibrated in this study, a Markov chain Monte Carlo method is used to estimate the MBA.

This section focuses on the updated parameters and, in turn, calculation of the reliability index and probability of failure in both states.

### 5.1 Results for the Undamaged State

Applying the MBA in the first health state, the calibrated parameters have been obtained, as shown in Table 3 and Fig. 9.

Table 3. The Likelihood and Posterior distribution for calibrated parameters in the undamaged state

Part	Before updating		After updating	
	Mean	Coefficient of Variation	Mean	Coefficient of Variation (%)
$E_{cBot}$	32 GPa	7.13	30.84 (GPa)	8.3
$E_{cWeb}$	32 GPa	7.13	32.69 (GPa)	2.9
$E_{cTop}$	32 GPa	7.13	33.67 (GPa)	5.2
$K_{Roller}$	$5 \times 10^7$ N/m	$9 \times 10$	$1.68 \times 10^7$ (N/m)	$2.02 \times 10^2$
$K_{Pin}$	$5 \times 10^7$ N/m	$9 \times 10$	$9.53 \times 10^7$ (N/m)	$3.82 \times 10^2$

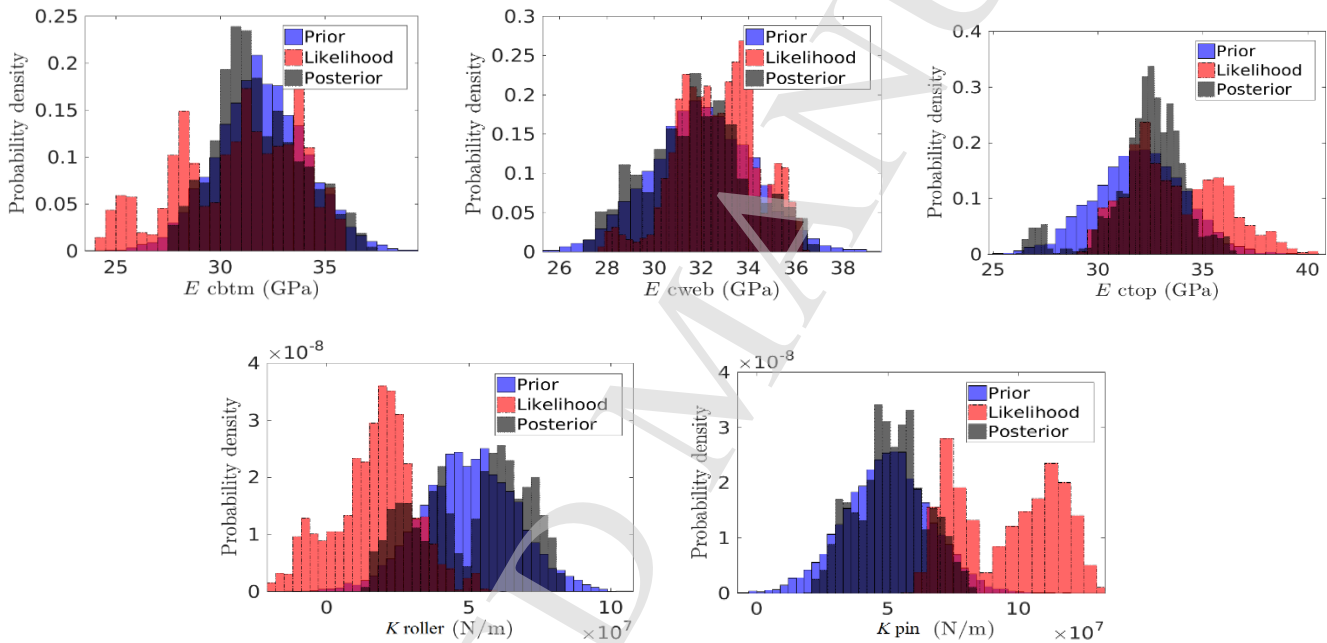


Figure 9. Calibrated parameters in undamaged state

No significant variations are observed in Young's moduli of the top slab and web after updating for the undamaged state. However, Young's modulus of the bottom slab is reduced, and this reduction can be considered a result of the minor cracks observed underneath the BGB. Regarding the boundary conditions, there is a noticeable change (60% drop) in the vertical spring stiffness at the roller support, implying that this was overestimated in the initial FE model. By obtaining the calibrated distribution of parameters for the undamaged state, the updated model is analysed with the aforementioned moving load cases to ascertain the maximum deflection and strain, which represent the effect of the loading action on the structure. Further, the structural resistance is obtained after the incremental analysis has caused the allowable maximum deflection to reach the specified limit. According to the observation of results, both maximum deflection and strain occur at the mid-span regardless of the load case used.

Fig. 10 shows the distribution of deflection and strain due to the load case M1600. The results for strain and deflection by applying MS1600 are shown in Table 4.

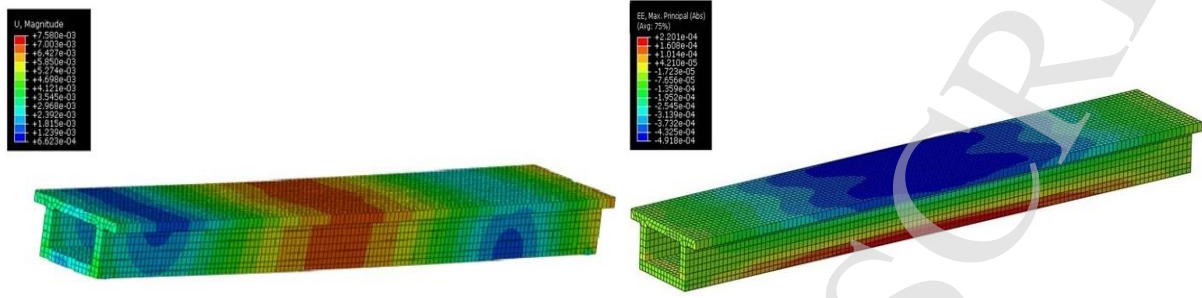


Figure 10. Max deflection (left) and Max normal strain (right) in BGB with applying the load case M1600

Table 4. Deflection and strain responses for load case MS1600 in undamaged state

	Strain (%)				Deflection (mm)			
	Before updating		After updating		Before updating		After updating	
	Mean	Standard Deviation	Mean	Standard Deviation	Mean	Standard Deviation	Mean	Standard Deviation
S1600 (Load action)	0.01175	0.0048	0.014	0.0041	8.24	1.62	9.41	1.55
M1600 (Load action)	0.00985	0.0041	0.01107	0.0038	6.67	1.48	7.72	1.41

Overall, the impact of S1600 load action is higher than that of M1600, which aligns with the previous observations of these loading cases. The distributions of deflection and strain before and after updating for the two loading cases are illustrated in Fig. 11. Even though the observed change is not significant at this health state, FEMU's significant role in updating the performance of structures is highlighted. In the next step, the reliability index ( $\beta$ ) and, in turn, the probability failure is calculated. The results of the reliability analysis for both states are shown in Table 7.

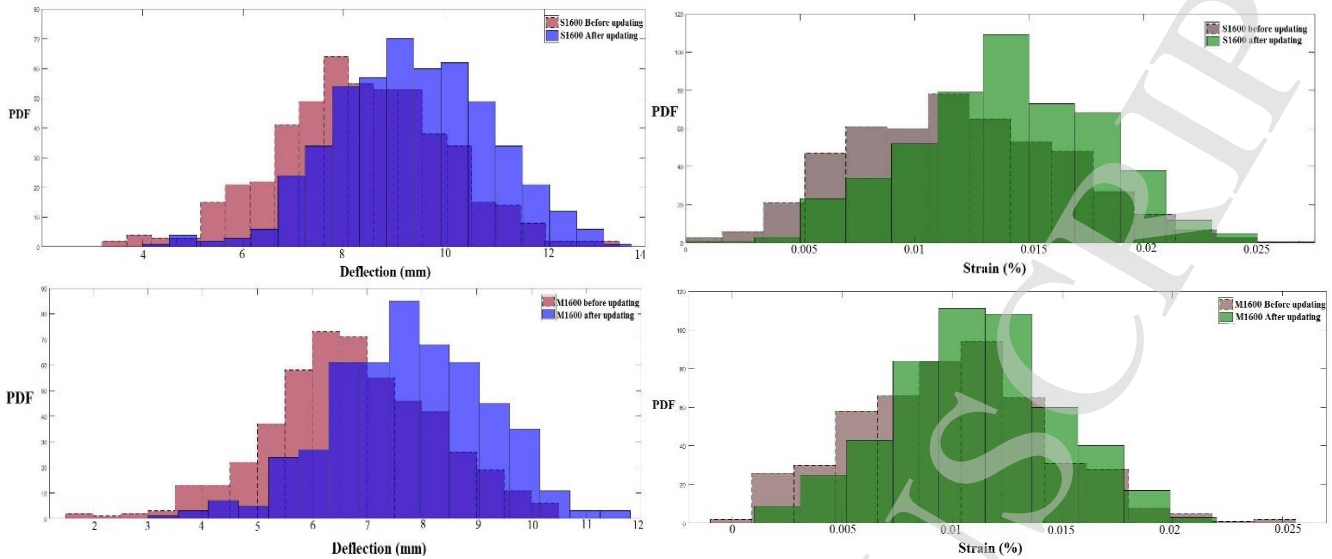


Figure 11. Results of deflection and strain for both loading cases in the undamaged state before and after updating

## 5.2 Results for the Damaged State

In this section, the MBA is applied for the damaged state, wherein some significant cracks are observed on the bottom slab and the webs of the BGB. It is worth mentioning that the number of calibrated parameters is reduced to three (i.e., Young's moduli of the concrete parts) because it is assumed that the applied impacts will not affect the boundary conditions of the damaged structure. The distributions of the updated parameters for the damaged state are shown in Fig. 12 and summarised in Table 5.

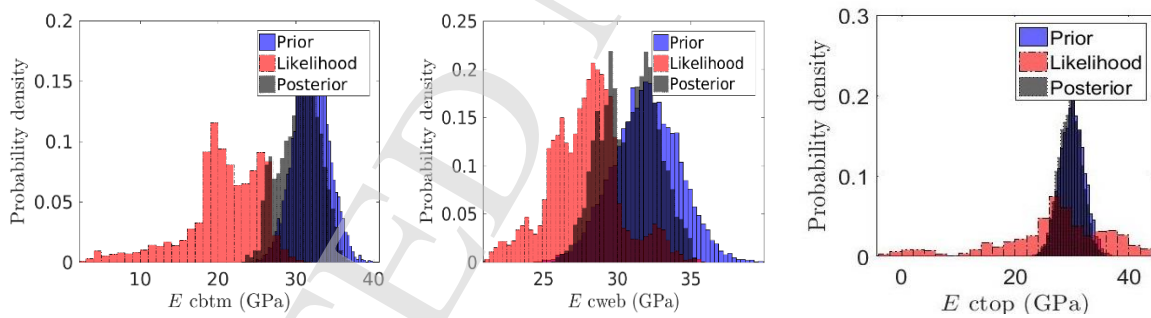


Figure 12. Calibrated parameters in undamaged state

Table 5. Distribution of calibrated parameters in damaged state

Part	Mean	Coefficient of Variation (%)
$E_{cBot}$	20.63 (GPa)	25.59
$E_{cWeb}$	27.82 (GPa)	5.99
$E_{cTop}$	30.54 (GPa)	35.45

As shown in Fig. 12, a significant change in Young's modulus of the bottom slab is observed for the damaged state, indicated by a reduction of about 40% and a new mean value of 20.63 GPa. Further, the decrease in Young's modulus of the web section is noticeable, showing an updated mean value of 27 GPa. The impact forces have little effect on the top slab, and its updated Young's modulus is almost the same as its initial value. It is worth noting that the reduction in Young's moduli for the bottom slab and the webs is well matched to the cracks observed in the damaged state. Additional results for the discrepancy function and predicting response from the MBA for both states can be found in Moravej et al. (2019a). The calibrated model of the damaged state with the updated parameter distributions is analysed to obtain the loading action on the structure as well as the structural resistance. The results for strain and deflection after updating are shown in Table 6 and Fig. 13.

Table 6. Deflection and strain responses for load case MS1600 in Damaged state

	Strain (%)		Deflection (mm)	
	Mean	Standard Deviation	Mean	Standard Deviation
S1600	7.20E-02	8.10E-03	17.02	2.03
M1600	5.79E-02	9.20E-03	14.8	1.87

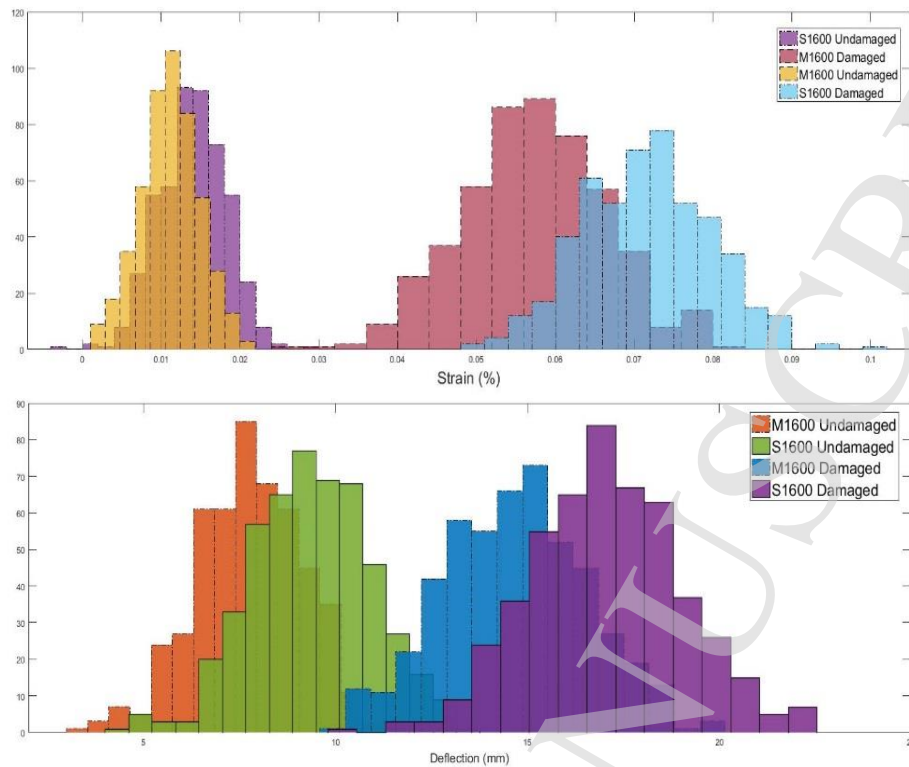


Figure 13. Updated distributions of strain and deflection in undamaged and damaged states

Fig. 13 highlights the noticeable variations in deflection and strain between both health states. It can also be inferred that the load effects in the damaged state are more scattered than those in the undamaged state. This is because the variation of the calibrated parameters in the damaged phase is greater compared with the undamaged phase. As explained in section 5.1, both the deflection and normal strain obtained from the loading case S1600 are more conservative than those obtained from M1600. However, in both loading cases, significant increases can be clearly identified in the deflection and strain of the BGB, which implies that the structure's performance has been compromised. Therefore, the reliability analysis is conducted to determine how far the current condition is from the expected safety margin. Since the input parameters are normal distributions, it is reasonable to expect that the output from the analysis follows the normal or lognormal distributions. The normality is also checked with the Kolmogorov–Smirnov test which implies the results obtained from FORM are reliable in this study. Fig. 14 shows the p-values of strain for M1600 and S1600, indicating a satisfaction of the 1% significance level. So, FORM is applied for both states, and the results are shown in Table 7 and Fig. 15.

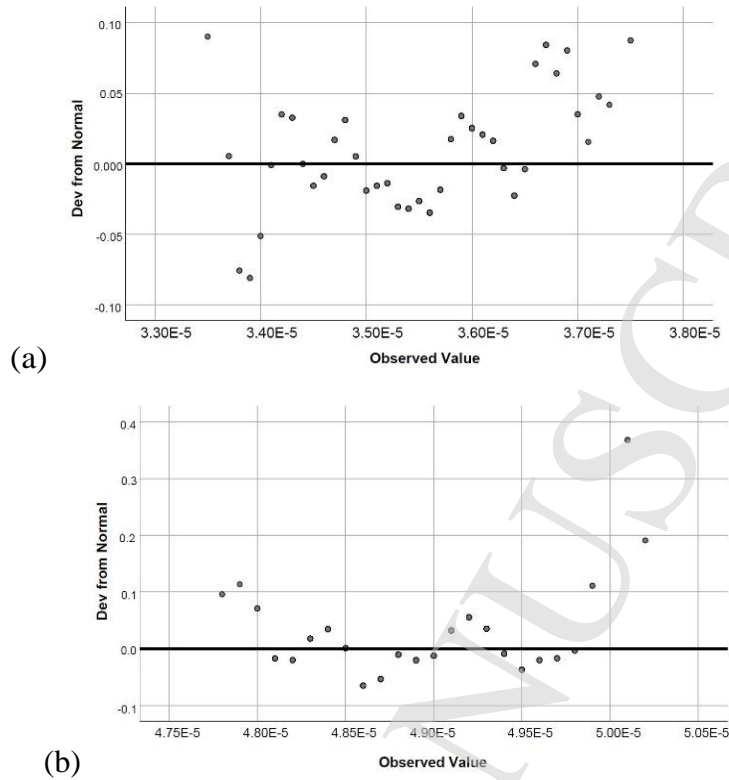


Figure 14. Kolmogorov–Smirnov test results for Strain (a) M1600, (b) S1600

Table 7. Results of Reliability index and Probability of failure for both loading actions in two states

	Strain (mm/mm)						Deflection (mm)					
	Undamaged Before Updating		Undamaged After Updating		Damaged After Updating		Undamaged Before Updating		Undamaged After Updating		Damaged After Updating	
	$\beta_1$	$P_f$	$\beta_2$	$P_f$	$\beta_3$	$P_f$	$\beta_4$	$P_f$	$\beta_5$	$P_f$	$\beta_6$	$P_f$
S1600	10.02	$10^{-9}$	9.96	$10^{-9}$	1.79	0.036	9.73	$10^{-9}$	9.41	$10^{-8}$	3.44	0.029
M1600	10.82	$10^{-11}$	10.78	$10^{-11}$	2.92	0.0017	11.71	$10^{-13}$	11.55	$10^{-13}$	4.92	$0.56 \cdot 10^{-5}$

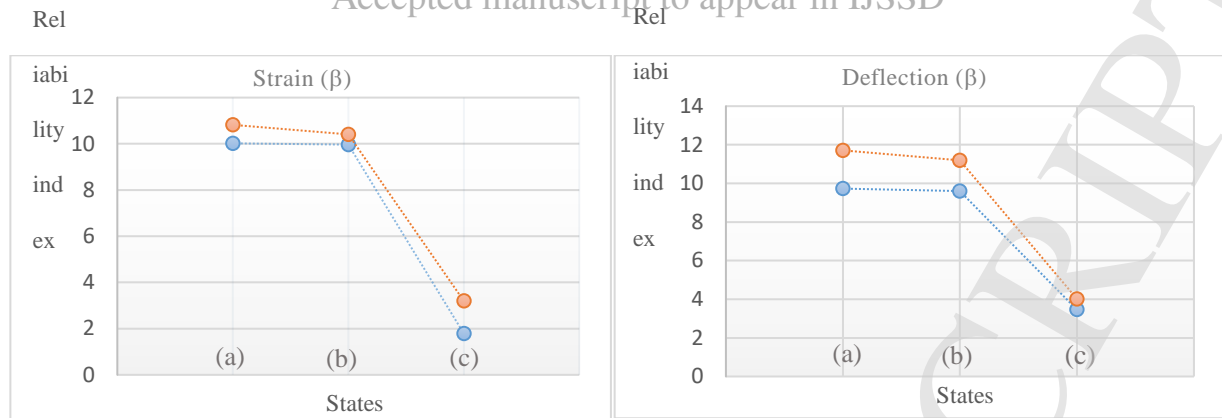


Figure 15. Results of Reliability index for S1600 (blue) and M1600 (orange) in: (a) undamaged before updating, (b) undamaged after updating and (c) damaged after updating

As can be seen in the above figure and table, the reliability index and probability of failure for both deflection and strain, even in the damaged state, still stay in the safe regions. However, the result for the damaged state illustrates noticeable drops in both reliability indices, which is feasible since the stiffness of BGB in the damaged state reduced by 40% and it led to the detectable cracks generated on the body of structure. According to Eurocode (EN 1990), the recommended reliability index for SLS is 1.5, corresponding to  $P_f = 6.7 \times 10^{-2}$ , for the design's operational life of 50 years. According to the results obtained in this study, the strain reliability index in S1600 is estimated as 1.79 for the damaged state (corresponding to  $P_f = 0.03673$ ), which is very close to the Eurocode's recommendation; this could be considered a threat to the performance of the structure.

## 6. Concluding Remarks

This paper has highlighted the important role of SHM data for updating the current understanding of structural capacity and for assessing structural safety. The study addressed the performance assessment of a BGB by integrating FEMU with reliability analysis. This study differed from most previous studies since it targeted the SLS — this is because keeping structural performance within the SLS limit not only saves a significant amount of money for maintenance actions but also rectifies the losses that prevent the functionality of infrastructure. For the first time, an approach was proposed that integrates MBA, the most comprehensive probabilistic FEMU technique, with reliability analysis to monitor point-in-time structural performance, which in turn improves the accuracy of structural maintenance decisions. Although this study focused on the point-in-time performance of the structure, this approach can be extended for cumulative-time reliability analysis (time-dependent reliability analysis) of in-service structures by providing statistical details, such as the occurrence rate of traffic loads. The structural assessment was performed in two phases, undamaged and damaged, which clearly illustrate the performance of the proposed approach. The study conducted a comprehensive structural assessment by applying two common loading cases in Australia and analysing the rate of change for two structural features, deflection and normal strain, to provide a more reliable judgement of structural safety. This work offers proof that FEMU is a robust tool for calibrating structural properties under uncertainty, while it is computationally efficient. Accordingly, the lifetime reliability of structures can be updated based on as-is evidence obtained from FEMU, which is more trustworthy



than using prediction techniques and nondestructive testing. Despite, in this study, FORM as the most common structural reliability technique has been applied, it is recommended that more accurate techniques, such as Monte Carlo be attempted in future research. In addition, this research can provide insights into a comprehensive assessment framework that can improve the current assessment approach, considering the absence of well-developed assessment guidelines in structural codes of practice.

## Acknowledgment

The research herein is part of Discovery Project DP160101764 funded by the Australian Government through the Australian Research Council (ARC). The authors also would like to thank DrShojaeddin Jamali for his assistance and guidance in preparing the initial FE model of the BGB and experimental data collection.

## Reference

ABAQUS, V., 2005. 6.5 Documentations, ABAQUS Inc.

Akgül, F. and Frangopol, D.M., 2004a. Bridge rating and reliability correlation: Comprehensive study for different bridge types. *Journal of Structural Engineering*, 130(7), pp.1063-1074.

Akgül, F. and Frangopol, D.M., 2004b. Lifetime performance analysis of existing prestressed concrete bridge superstructures. *Journal of Structural Engineering*, 130(12), pp.1889-1903.

Akgül, F. and Frangopol, D.M., 2005. Lifetime performance analysis of existing reinforced concrete bridges. I: Theory. *Journal of infrastructure systems*, 11(2), pp.122-128.

American Association of State Highway and Transportation Officials, 2010. *AASHTO LRFD Bridge Design Specifications: US Customary Units*. American Association of State Highway and Transportation Officials.

American Society of Civil Engineers, 2010. *Transactions of the American Society of Civil Engineers 2009*

Arendt, P.D., Apley, D.W., and Chen, W., 2012a. Quantification of model uncertainty: Calibration, model discrepancy, and identifiability. *Journal of Mechanical Design*, 134(10), p.100908.

Arendt, P.D., Apley, D.W., Chen, W., Lamb, D. and Gorsich, D., 2012b. Improving identifiability in model calibration using multiple responses. *Journal of Mechanical Design*, 134(10), p.100909.

Baraldi, P., Podofillini, L., Mkrtychyan, L., Zio, E. and Dang, V.N., 2015. Comparing the treatment of uncertainty in Bayesian networks and fuzzy expert systems used for a human reliability analysis application. *Reliability Engineering & System Safety*, 138, pp.176-193.

Bichon BJ, Eldred MS, Swiler LP, Mahadevan S, McFarland JM (2008) *Efficient global reliability analysis for nonlinear implicit performance functions*. AIAA J 46(10):2459–2468

Bolton, S., 2019. Speculation is cause of tower disasters. *Green Left Weekly*, (1229), p.3.

Conde, B., Eguía, P., Stavroulakis, G.E. and Granada, E., 2018. Parameter identification for damaged condition investigation on masonry arch bridges using a Bayesian approach. *Engineering Structures*, 172, pp.275-284.

Dubourg V, Sudret B, Deheeger F (2013) *Metamodel-based importance sampling for structural reliability analysis*. Probabilistic Eng Mech 33:47–57

Du, X., 2005. First order and second reliability methods. *Probabilistic engineering design*, pp.1-33.

Echard B, Gayton N, Lemaire M (2011) AK-MCS: *an active learning reliability method combining Kriging and Monte Carlo simulation*. Struct Saf 33(2):145–154

Echard B, Gayton N, Lemaire M, Relun N (2013) *A combined importance sampling and kriging reliability method for small failure probabilities with time-demanding numerical models*. Reliability Engineering & System Safety 111:232–240

Enright, M.P. and Frangopol, D.M., 1998. Service-life prediction of deteriorating concrete bridges. *Journal of Structural engineering*, 124(3), pp.309-317.

Estes, A.C. and Frangopol, D.M., 1999. Repair optimization of highway bridges using system reliability approach. *Journal of structural engineering*, 125(7), pp.766-775. Eurocode, C.E.N., 1990. 0: Basis of structural design. *European Standard EN*, 2002.

Friswell, M. and Mottershead, J.E., 2013. Finite element model updating in structural dynamics (Vol. 38). *Springer Science & Business Media*.

Hasofer, A.M. and Lind, N.C., 1974. Exact and invariant second-moment code format. *Journal of the Engineering Mechanics division*, 100(1), pp.111-121.

Harris, H.G. and Sabnis, G., 1999. *Structural modeling and experimental techniques*. CRC press.

Hendawi, S. and Frangopol, D.M., 1994. System reliability and redundancy in structural design and evaluation. *Structural safety*, 16(1-2), pp.47-71.

Hosser, D., Windzio, M. and Greve, W., 2008. Guilt and shame as predictors of recidivism: A longitudinal study with young prisoners. *Criminal Justice and Behavior*, 35(1), pp.138-152.

Jamali, S, Chan, TH, Nguyen, A, et al. (2018) Reliability-based load-carrying capacity assessment of

bridges using structural health monitoring and nonlinear analysis. *Structural Health Monitoring* 18(1): 20–34.

Jesus, A., Brommer, P., Westgate, R., Koo, K., Brownjohn, J. and Laory, I., 2019. Bayesian structural identification of a long suspension bridge considering temperature and traffic load effects. *Structural Health Monitoring*, 18(4), pp.1310-1323.

Jesus, A., Brommer, P., Westgate, R., Koo, K., Brownjohn, J. and Laory, I., 2019. Modular Bayesian damage detection for complex civil infrastructure. *Journal of Civil Structural Health Monitoring*, 9(2), pp.201-215.

Jesus, A., Brommer, P., Zhu, Y. and Laory, I., 2017. Comprehensive Bayesian structural identification using temperature variation. *Engineering Structures*, 141, pp.75-82.

Jesus, A.H., Dimitrovová, Z. and Silva, M.A., 2014. A statistical analysis of the dynamic response of a railway viaduct. *Engineering Structures*, 71, pp.244-259.

Jiang, Z., Chen, W., Fu, Y. and Yang, R.J., 2013. Reliability-based design optimization with model bias and data uncertainty. *SAE International Journal of Materials and Manufacturing*, 6(3), pp.502-516.

Kennedy, M.C. and O'Hagan, A., 2001. Bayesian calibration of computer models. *Journal of the Royal Statistical Society: Series B (Statistical Methodology)*, 63(3), pp.425-464.

Kodikara, K.A.T.L., Chan, T.H., Nguyen, T. and Thambiratnam, D.P., 2016. Model updating of real structures with ambient vibration data. *Journal of Civil Structural Health Monitoring*, 6(3), pp.329-341.

Lophaven, S.N., Nielsen, H.B. and Søndergaard, J., 2002. DACE-A *Matlab Kriging toolbox*, version 2.0.

Moravej, H., Jamali, S., Chan, T. and Nguyen, A., 2017. Finite element model updating of civil engineering infrastructures: A literature review. In Proceedings of the 8th International Conference on Structural Health Monitoring of Intelligent Infrastructure 2017 (pp. 1-12). *International Society for Structural Health Monitoring of Intelligent Infrastructure (ISHMII)*.

Moravej, H., Chan, T.H., Nguyen, K.D. and Jesus, A., 2019a. Vibration-based Bayesian model updating of civil engineering structures applying Gaussian process metamodel. *Advances in Structural Engineering*, p.1369433219858723.

Moravej, H., Chan, T.H., Nguyen, K.D. and Jesus, A., 2019b. Application of Gaussian process metamodel in structural finite element model updating applying dynamic measured data. In *5th International Conference on Smart Monitoring, Assessment and Rehabilitation of Civil Structures*, 27-29 Aug 2019, Potsdam, Germany.

Moravej, H., Vafaei, M. and Abu Bakar, S., 2016. Seismic performance of a wall-frame air traffic control tower. *Earthquakes and Structures*, 10(2), pp.463-482.

Moravej, H. and Vafaei, M., 2019. Seismic Performance Evaluation of an ATC Tower through Pushover Analysis. *Structural Engineering International*, 29(1), pp.144-149.

Mori, Y. and Ellingwood, B.R., 2006. Reliability assessment of reinforced concrete walls degraded by aggressive operating environments. *Computer-Aided Civil and Infrastructure Engineering*, 21(3), pp.157-170.

Moses, F., 1982. System reliability developments in structural engineering. *Structural Safety*, 1(1), pp.3-13.

Moses, F. and Rashedi, M.R., 1983, June. The application of system reliability to structural safety. *Proceedings, 4th International Conference-Applications of Statistics and Probability in Soil and Structural Engineering*. Pitagora Editrice, Bologna, Italy, Florence, Italy 1983pp (Vol. 573, p. 584).

Nannapaneni, S. and Mahadevan, S., 2016. *Reliability analysis under epistemic uncertainty*. Reliability Engineering & System Safety, 155, pp.9-20.

Nguyen, A., Chan, T., Thambiratnam, D., Kodikara, K.A.T.L., Le, N.T. and Jamali, S., 2017. Output-only modal testing and monitoring of civil engineering structures: Instrumentation and test management. In Proceedings of the 8th International Conference on Structural Health Monitoring of Intelligent Infrastructure 2017 (pp. 1134-1145). *International Society for Structural Health Monitoring of Intelligent Infrastructure (ISHMII)*.

Nguyen, A., Kodikara, K.A.T.L., Chan, T.H.T. and Thambiratnam, D.P., 2018. Toward effective structural identification of medium-rise building structures. *Journal of Civil Structural Health Monitoring*, 8(1), pp.63-75.

Nguyen, A., Kodikara, K.T.L., Chan, T.H. and Thambiratnam, D.P., 2019. Deterioration assessment of buildings using an improved hybrid model updating approach and long-term health monitoring data. *Structural Health Monitoring*, 18(1), pp.5-19.

Nowak, A.S., 1999. *Calibration of LRFD bridge design code* (No. Project C12-33 FY'88-'92).

Okasha, N.M. and Frangopol, D.M., 2010. Advanced modeling for efficient computation of life-cycle performance prediction and service-life estimation of bridges. *Journal of Computing in Civil Engineering*, 24(6), pp.548-556.

Okasha, N.M., Frangopol, D.M. and Orcesi, A.D., 2012. Automated finite element updating using strain data for the lifetime reliability assessment of bridges. *Reliability Engineering & System Safety*, 99, pp.139-150.

Pan, H. and McMichael, D., 1998, July. Fuzzy causal probabilistic networks-a new ideal and practical inference engine. In *Proc. 1st International Conference on Multisource-Multisensor Information Fusion* (pp. 6-8).

Pan, H., Xi, Z. and Yang, R.J., 2016. Model uncertainty approximation using a copula-based approach for reliability based design optimization. *Structural and Multidisciplinary Optimization*, 54(6), pp.1543-1556.

Pathirage, T.S., 2017. *Identification of prestress force in prestressed concrete box girder bridges using vibration based techniques* (Doctoral dissertation, Queensland University of Technology).

Simoen, E., De Roeck, G. and Lombaert, G., 2015. Dealing with uncertainty in model updating for damage assessment: A review. *Mechanical Systems and Signal Processing*, 56, pp.123-149.

Standards Australia, 2017. AS 5100.1-2017: Bridge Design—Scope and General Principles.

Structural Vibration Solutions A/S (2011) SVS-ARTEMIS extractor-release 5.3, user's manual. Aalborg: *Structural Vibration Solutions A/S*.

Tang, K. and Melchers, R.E., 1988. Incremental formulation for structural reliability analysis. *Civil Engineering Systems*, 5(3), pp.153-158.

Thoft-Christensen, P. and Murotsu, Y., 1986. Reliability Analysis of Structural Systems by the  $\beta$ —Unzipping Method. *In Application of Structural Systems Reliability Theory* (pp. 143-214). Springer, Berlin, Heidelberg.